Fermi surfaces and electronic structure of the Heusler alloy $Co_2TiSn$



2006 J. Phys.: Condens. Matter 18 2897

(http://iopscience.iop.org/0953-8984/18/10/012)

INSTITUTE OF PHYSICS PUBLISHING JOURNAL OF PHYSICS: CONDENSED MATTER

J. Phys.: Condens. Matter **18** (2006) 2897–2903 doi:10.1088/0953-8984/18/10/012

# Fermi surfaces and electronic structure of the Heusler alloy $Co_2TiSn$

**M C Hickey[1,2], A Husmann[2], S N Holmes[2] and G A C Jones[1]**

[1] Department of Physics, Cavendish Laboratory, University of Cambridge, J J Thompson Avenue, Cambridge, CB2 OHE, UK
[2] Toshiba Research Europe, Cambridge Research Laboratory, 260 Cambridge Science Park, Milton Road, Cambridge, CB4 OWE, UK

E-mail: mch40@cam.ac.uk

Received 13 January 2006
Published 20 February 2006
Online at stacks.iop.org/JPhysCM/18/2897

**Abstract**

The electronic structure of the Heusler alloy $Co_2TiSn$ is investigated here, with particular attention paid to its potential as a half-metallic ferromagnet. *Ab initio* calculations are performed using a plane wave pseudopotential code in the framework of density functional theory. These accurate calculations are done with convergence tolerances of $10^{-5}$ and $10^{-4}$ eV on the total energy and Fermi energy, respectively. The alloy is found not to be a half-metal. Minority spin electrons undergo distinctly hole-like dispersion at the $\Gamma$ point in $k$ space while the majority spin bands are metallic with a multiply connected tube-like Fermi surface. Further, the computed minority band gap and spin polarization at the Fermi level are larger when the calculation is performed using the generalized gradient approximation.

From the vast family of full Heusler alloys based on the formula $X_2YZ$, there are a subset of alloys which are predicted to be half-metallic [1]. These ternary metals are interesting as they promise a great deal in the field of spintronics. An imbalance between spin up and down electrons is required to generate spin polarized currents for device applications that exploit spin. Half-metallic materials have recently been categorized in a new classification scheme [2] which incorporates systems which have itinerant majority electrons but localized or heavy minority spin carriers at the Fermi level ($E_F$). Several Co-based full Heusler alloys have been theoretically predicted [1, 3–5] to fall into the type $I_A$ half-metal group of this categorization scheme, for which the density of states of the minority spins is zero at $E_F$ and the conduction is mediated through majority spin carriers. So far, the most theoretically and experimentally proven half-metallic ferromagnet is $CrO_2$ [2] for which point contact Andreev reflection experiments have shown a transport spin polarization of 96 ± 2% [6]. Recently, calculations have shown half-metallicity in the Heusler alloy $Co_2CrAl$ [7, 8] with a spin band gap of about 0.48 eV which is robust against uniform strain of up to 3% and a tetragonal

  

lattice distortion of between $-2\%$ and $+2\%$. In this work, we focus on one of the Heusler alloys without Mn—$Co_2TiSn$—and attempt to elucidate its spin resolved electronic structure in terms of density of states, band structure and Fermi surfaces using *ab initio* methods and pseudopotentials.

Early electronic structure calculations done by Ishida *et al* [9] for the alloys $Co_2TiSn$ and $Co_2TiAl$ used the spline augmented plane wave (SAPW) method to evaluate the atomic site contributions to the total orbital angular momentum. They showed that the band structure is strongly spin polarized with a density of states dominated by Co d electrons at $E_F$ with an almost entirely flat band of d electrons contributing to the minority density of states at $E_F$. Recently, Galanakis *et al* [15], using the full potential screened Korringa–Kohn–Rostoker Green's function method incorporating LSDA, found that the alloys $Co_2TiSn$ and $Co_2TiAl$ were not half-metallic. Mohn *et al* [10] also reached similar conclusions using the LSDA scheme. Yamasaki *et al* [11] have performed linear muffin-tin orbital calculations with the atomic sphere approximation (LMTO + ASA) on $Co_2TiSn$ and concluded that the system was not half-metallic in the LSDA scheme. However, Lee *et al* [12] have since performed augmented plane wave calculations using linear orbitals (APW +LO) for alloys of the form $Co_2TiX$ and have demonstrated that they are half-metallic with integer total magnetic moment using the GGA exchange–correlation scheme. As it stands, the calculated properties of $Co_2TiSn$ have yielded a slightly inconsistent picture and clearer insight is sought as regards how to theoretically classify this alloy in the absence of direct experimental evidence for half-metallicity. In this work, we use the *ab initio* plane wave basis code CASTEP [13] which was developed at the Cavendish Laboratory and uses ultrasoft pseudopotentials in the framework of density functional theory. The exchange–correlation potential is treated using both local spin density approximation (LSDA) and the generalized gradient approximation (GGA) methods in separate calculations. For the GGA case, we use the revised approximation of the Perdew–Burke–Ernzerhof [14] scheme, which extrapolates the slowly varying electron density approximation to account for first-and second-order spin density gradients. The accuracy with which the linear response of the uniform gas is constructed is retained. We use these methods to outline subtle differences in the density of states and in particular the size of the minority band gap. We compute the band structure for spin up and down electrons and seek further information about the band properties by generating the Fermi surfaces for both spin types.

$Co_2TiSn$ crystallizes in the $L2_1$ cubic structure with the space group $Fm3m$ and can be thought of as two interpenetrating fcc sublattices—one of which is entirely composed of Co atoms. The positions of the Co atoms are $\pm(\frac{1}{4}, \frac{1}{4}, \frac{1}{4})$, while the Ti and Sn atoms are located at $(\frac{1}{2}, \frac{1}{2}, \frac{1}{2})$ and $(0, 0, 0)$ in Wyckoff coordinates respectively. This defines the formula unit. The lattice constant is measured to be 6.073 Å from x-ray measurements on bulk samples. This Heusler alloy is lattice matched to the narrow gap III–V semiconductors InAs, GaSb and AlSb, which paves the way for future spin injection hybrid devices using these materials. Spin manipulation in these narrow gap materials can be facilitated by the effects of spin–orbit coupling, such as a large Rashba effect and Landé $g$-factors ($-15$ for InAs). The saturated bulk magnetic moment from magnetization measurements [16] is 1.96 $\mu_B$ per formula unit (f.u.). The magnetic moment has been measured to be close to an integer number of Bohr magnetons which indicates compliance with the Slater–Pauling curve for these Heusler alloys [15]: $M_T = Z_T - 24$ (where $M_T$ and $Z_T$ are the total magnetic moment per formula unit and the number of valence electrons, respectively). Compliance with the Slater–Pauling curve satisfies one of the criteria for half-metallicity.

The CASTEP code solves the Kohn–Sham equations self-consistently using a plane wave basis set in the framework of density functional theory. The atomic potentials for Co, Ti and Sn

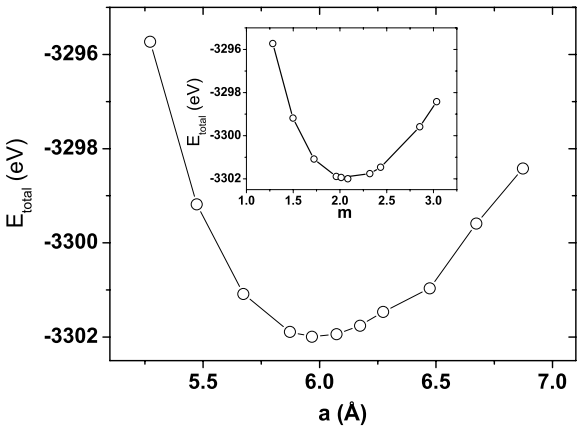


**Figure 1.** Equilibrium lattice constant $a$ (Å) and spin density $m = |n_\uparrow - n_\downarrow|$ obtained by total energy minimization in the LDA approximation for $Co_2TiSn$.

were taken from a library of ultrasoft pseudopotentials. The electronic bands were calculated for 26 valence electrons with the configurations $3d^74s^2$ (Co), $3d^24s^2$(Ti) and $5s^25p^2$(Sn). The method of using a plane wave basis set in conjunction with pseudopotentials is similar to the orthogonalized plane wave approach. In the latter method, the valence states are orthogonalized to the core states, which is equivalent to the addition of repulsive term to the crystal potential (making it a pseudopotential). The plane wave pseudopotential method can be powerful for predicting macroscopic quantities of simple metals as the pseudopotential has a small number of adjustable parameters which are empirically set by experimental data. Further, the resulting wavefunctions are well suited to interpolating the band energies at many points which are required for Fermi surfaces. The plane wave basis cut-off energy was increased to 500 eV to ensure convergence of the total energy ($E_T$) and $E_F$. The convergence tolerances on $E_T$ and $E_F$ are $10^{-5}$ and $10^{-4}$ eV respectively. The computed value of $E_T$ was minimized with respect to the lattice constant and spin density ($m = |n_\uparrow - n_\downarrow|$). By minimizing the total energy with respect to the lattice volume, an equilibrium lattice constant of $a = 6.070 \pm 0.005$ Å was predicted (see figure 1) which agrees well with experiment. The GGA method gives a slightly larger equilibrium lattice constant: $a = 6.083 \pm 0.005$ Å. The equilibrium spin density was found to be $m = 2.00 \pm 0.02$ by total energy minimization (see figure 1) which gives the total magnetic moment per f.u. in Bohr magnetons.

The electronic band structure of $Co_2TiSn$ for spin $\uparrow$ and $\downarrow$ electrons was computed using 256 $k$-points along the symmetry path $\Gamma \to X \to W \to L \to \Gamma \to U \to X' \to W \to K \to L$ in the first Brillouin zone of the fcc lattice. In order to calculate the density of states and to construct the Fermi surfaces, an irreducible wedge of the Brillouin zone was made into a $10 \times 10 \times 10$ Monkhorst–Pack grid [17]. The density of states is then computed for both spin types and a partial density of states is constructed by projecting the plane wave states onto atomic orbital wavefunctions [18].

The LSDA density of states (see figure 2) for this Heusler alloy shows a minority spin band gap of $\Delta E_\downarrow = 0.47 \pm 0.06$ eV with a Fermi level spin polarization $\Pi = (n_\uparrow - n_\downarrow)/(n_\uparrow + n_\downarrow) = 0.57$, which shows that the alloy is not half-metallic (type $I_A$ [2]). There are many sharp features in the density of states which arise due to the presence of flat Co d bands. Furthermore, the GGA method (see figure 2) gives a higher value of $\Delta E_\downarrow$ of $0.59 \pm 0.07$ eV and gives $\Pi = 0.76$. Thus, the calculated half-metallic properties of $Co_2TiSn$ are sensitive to the exchange–correlation scheme used, which is an important subtlety in predicting whether such materials are in fact

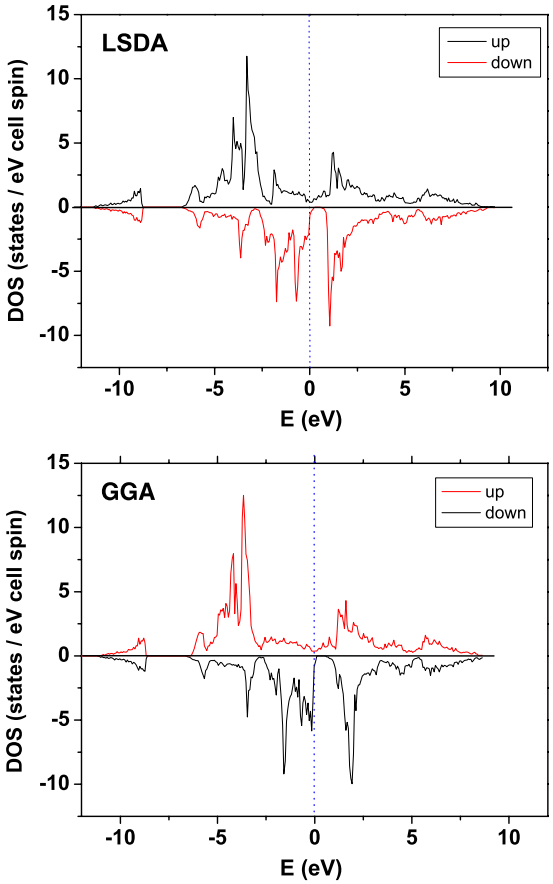


**Figure 2.** Spin resolved density of states for $Co_2TiSn$ obtained using the LSDA and GGA exchange–correlation schemes. The minority spin band gap is larger for the GGA case.

true half-metals. In the GGA case, the exchange energy for the Co d states is enhanced by the inclusion of charge density gradient terms in the energy density functional. Further, the GGA equilibrium lattice constant is larger, making the electron gas more dilute, and hence the exchange energy competes more strongly with the kinetic energy. In the work presented here, the LSDA approximation predicts the equilibrium lattice constant more accurately as compared with the GGA method, which slightly overestimates it.

The spin resolved band structure is plotted in figure 3. The majority spin bands exhibit itinerant Co d bands cutting across the Fermi level, while the higher Ti d bands are unoccupied and hybridize with the Co d orbitals of similar symmetry. For the minority spin bands, hole-like d states of $\Gamma_{25}(t_{2g})$ symmetry rise up to the Fermi level and give a sharp feature in the density of states very close to $E_F$. The crystal field splits the orbitals of $\Gamma_{25}(t_{2g})$ and $\Gamma'_{12}(e_g)$ symmetry and this splitting controls the size of the minority band gap where the bandwidth of the d orbitals is narrow (see figure 3).

The Fermi surface (see figure 4) of the majority spins shows a tube-like sheet with arms extending out to the X points ($\frac{2\pi}{a}\langle 001\rangle$) in the Brillouin zone. The minority Fermi surface is a small pea-like structure at the $\Gamma$ point in the Brillouin zone which reflects the population of heavy electronic states which transform according to the $\Gamma_{25}(t_{2g})$ symmetry representation.

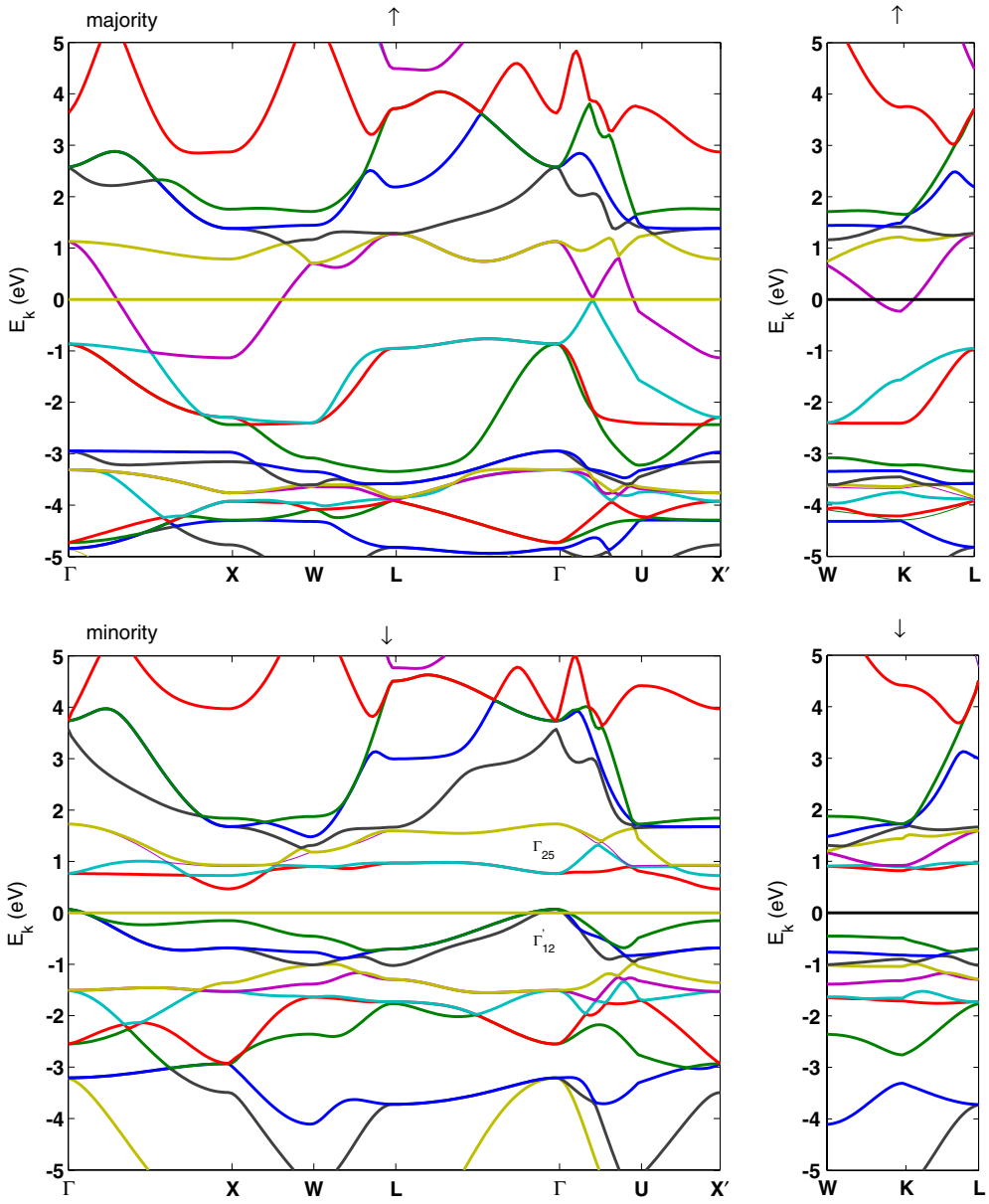


**Figure 3.** Spin resolved band structure for $Co_2TiSn$ obtained using the LSDA method. Note the hole-like dispersion at the Γ point for spin ↓ electrons and the itinerant d band spin ↑ states.

It is useful to consider again how the total energy $E_T$ varies with the lattice constant and magnetic ordering parameter $m$. The former relationship is well described by the Birch–Murnaghan equation of state [19], from which the elastic bulk modulus can be found. The $E_T(m)$ plot is interesting because it also points towards a parabolic dependence of $E_T$ on the spin ordering parameter in the ferromagnet. This implies that the alloy possess a magnetostatic bulk modulus, which is a positive quantity and plays the role of a magnetic analogue to the mechanical elastic bulk modulus.

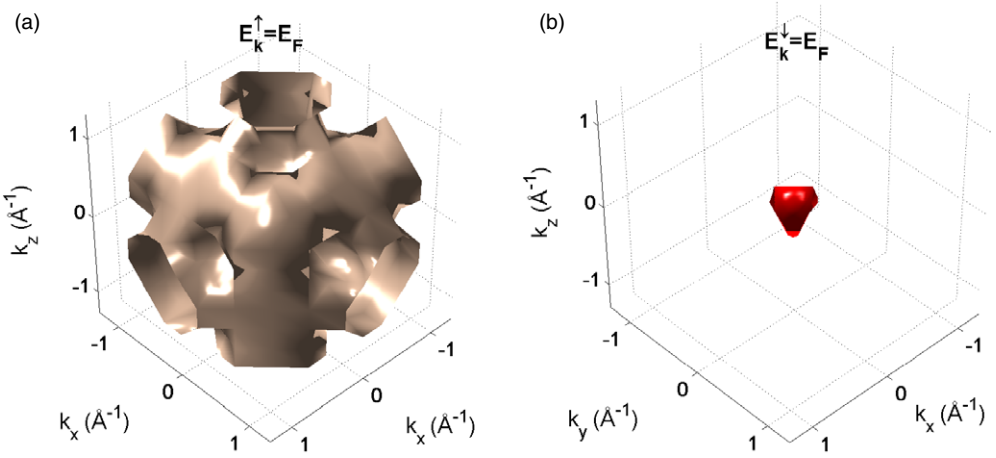


**Figure 4.** Fermi surfaces for majority (a) and minority (b) spin bands. The tube-like majority Fermi surface arises from the itinerant Co d electrons.

The electronic structure properties predicted here do not describe $Co_2TiSn$ as a true type I half-metallic ferromagnet in either the LSDA or the GGA schemes. Nevertheless, it can be concluded that in the GGA approximation, the minority band gap and bulk spin polarization at $E_F$ are larger. As indicated previously, the minority band gap is largely controlled by the crystal field splitting of the minority Co d states with symmetry $\Gamma_{25}(t_{2g})$ and $\Gamma'_{12}(e_g)$. In the GGA calculation, charge inhomogeneity is more strongly favoured than in the LSDA case, which yields a stronger crystal field, pushing these minority d band states further apart. The larger equilibrium lattice constant predicted using the GGA scheme results in a reduction in the Co minority d band hopping strength which gives a narrower d bandwidth (on either side of $E_F$). In the presence of a given crystal field splitting, this yields a wider calculated minority band gap. In both cases, the character of the minority spin bands is largely dominated by carriers which undergo hole-like dispersion about the $\Gamma$ point, indicating at least a candidate for type III half-metallic ferromagnetism (for which the majority and minority bands are itinerant and localized respectively). Although the density of states of the majority spin band is small, it is strongly metallic with a tube-like Fermi surface. In this alloy, $E_F$ lies at the edge of the minority spin gap and the density of states of the minority spins goes to zero over a range of energies equal to this gap. The majority spin density of states is finite over this range, which leads to vastly different electron lifetimes for each spin type under excitation above $E_F$ (hot electron lifetimes). The possibility of exploiting such a robust property in a hot electron spin filtering device could be envisaged [20]. In summary, the electronic properties of $Co_2TiSn$ calculated here give a minority spin band gap of $\Delta E_{\downarrow} = 0.47 \pm 0.06$ eV with a Fermi level spin polarization $\Pi = 0.57$ using the LSDA method. Using the GGA exchange–correlation method, $\Delta E_{\downarrow}$ is predicted to be $0.59 \pm 0.07$ eV but the equilibrium lattice constant is slightly overestimated. In both cases, majority spin carriers are metallic with a multiply connected tube-like Fermi surface, while the minority spin carriers undergo hole-like dispersion in a broad d band rising up to the Fermi level. Thus, $Co_2TiSn$ is predicted here to be a candidate for showing type III half-metallicity (a transport half-metal) according to a new classification scheme. As a final remark, spin–orbit coupling is almost always neglected in these calculations. In the case of the properties of $Co_2TiSn$ calculated here, this relativistic correction to the band structure may be relevant because of the location of $E_F$ relative to the minority band gap. Spin–orbit

coupling as a perturbation on the calculated bands here will more strongly affect the narrower d bands. The inclusion of spin–orbital coupling in these alloys generally will lift the degeneracy of the d band orbitals of $\Gamma'_{12}$ and $\Gamma_{25}$ symmetry. As these states get pushed further apart, the minority spin gap will be reduced, indicating that a more accurate description of the spin resolved electronic properties of this Heusler alloy would require spin–orbital coupling to be included in future work.

## Acknowledgments

The authors wish to gratefully acknowledge P D Haynes of the Cavendish Laboratory for his advice on performing the calculations and useful discussions. M C Hickey would like to acknowledge the Semiconductor Physics group at the Cavendish Laboratory, Cambridge, and the Cambridge European Trust for funding. We would like to thank G G Lonzarich for helpful discussions.

## References

[1] de Groot R A, Mueller F M, van Engen P G and Buschow K H J 1983 *Phys. Rev. Lett.* **50** 2024
[2] Coey J M D and Venkatesan M 2002 *J. Appl. Phys.: Appl. Phys.* **91** 8345
[3] de Groot R A and Buschow K H J 1986 *J. Magn. Magn. Mater.* **54** 1377
[4] Fujii S, Sugimura S, Ishida S and Asano S 1990 *J. Phys.: Condens. Matter* **2** 8583
[5] Otto M J, van Woerden R A M, van der Valk P J, Wijngaard J, van Bruggen C F and Haas C 1989 *J. Phys.: Condens. Matter* **3** 2351
[6] Soulen R J Jr, Byers J M, Osofsky M S, Nadgorny B, Ambrose T, Cheng S F, Broussard P R, Tanaka C T, Nowak J, Moodera J S, Barry A and Coey J M D 1998 *Science* **282** 85
[7] Zhang M, Liu Z H, Hu H N, Liu G D, Cui Y T, Chen J L, Wu G H, Zhang X X and Xiao G 2003 *J. Magn. Magn. Mater.* **277** 130
[8] Block T, Carey M J, Gurney B A and Jepsen O 2004 *Phys. Rev.* B **70** 205114
[9] Ishida S *et al* 1982 *J. Phys. F: Met. Phys.* **12** 1111
[10] Mohn P, Blaha P and Schwarz K 1995 *J. Magn. Magn. Mater.* **140** 283
[11] Yamasaki A, Imada S, Arai R, Utsunomiya H, Suga S, Muro T, Saitoh Y, Kanomata T and Ishida S 2002 *Phys. Rev.* B **65** 104410
[12] Lee S C, Lee T D, Blaha P and Schwarz K 2005 *J. Appl. Phys.* **97** 10C307
[13] Segall M D, Lindan P J D, Probert M J, Pickard C J, Hasnip P J, Clark S J and Payne M C 2002 *J. Phys.: Condens. Matter* **14** 2717
[14] Perdew J P, Kurth S, Zupan A and Blaha P 1999 *Phys. Rev. Lett.* **82** 2544
[15] Galanakis I, Dederichs P H and Papanikolaou N 2002 *Phys. Rev.* B **66** 174429
[16] van Engen P G, Buschow K H J and Ermann M 1983 *J. Magn. Magn. Mater.* **30** 374
[17] Monkhorst H J and Pack J D 1976 *Phys. Rev.* B **13** 5188
[18] Sanchez-Portal D *et al* 1996 *J. Phys.: Condens. Matter* **8** 3859
[19] Murnaghan F D 1944 *Proc. Natl. Acad. Sci.* **30** 244
[20] Vlutters R, van 't Erve O M J, Jansen R, Kim S D, Lodder J C and Vedyayev A 2002 *Phys. Rev.* B **65** 024416